

〈논 문〉 SAE NO. 97370092

Intake Valve Temperature Effect on the Mixture Preparation in a SI Engine During Warm-up

신 영 기*
Y. G. Shin

ABSTRACT

A heat transfer model of the intake valve in a spark ignition engine is presented, which is calibrated with a number of the valve temperature profiles measured during engine warm-up for the gaseous fuel(propane). The valve is divided into four identical elements for which the assumption of lumped thermal mass is applied. The calibration is made so that the difference between the measured and simulated valve temperatures becomes minimal. Then, the model is applied to the cases of the liquid fuel(indolene) to estimate the amount of the liquid fuel vaporized from the intake valve by assuming that fuel evaporation accounts for the deficit of the heat balance budget. The results of the model show quantitative contribution of each heat transfer source to the heat balance. The behavior of the calculated mass fraction of the fuel vaporized from the intake valve explains how the liquid fuel evaporates during engine warm-up, indicating the important role of the intake valve during the early stage of engine warm-up. The mass fraction at warmed-up conditions is closely related with the fraction directly targeted on the valve back by the fuel spray geometry.

Keywords : Intake Valve, Mixture Preparation, Modeling, Heat Transfer, Engine

Nomenclature

C : thermal conductivity
m : mass

T : temperature
 \dot{q} : heat
p : pressure
D : diameter
 \dot{m} : mass flow rate
 χ : mass fraction

*정회원, Massachusetts Institute of Technology
Sloan Automotive Laboratory, Cambridge MA,
U.S.A.

Greek

- γ : specific heat ratio
 μ : dynamic viscosity
 ρ : density

Subscripts

- v : valve
 evap : evaporation
 seat : valve seat
 cyl : in-cylinder
 back : backflow
 fg : phase transition
 sat : saturation
 p : piston
 r : reference
 m : motoring
 d : displacement

1. Introduction

The Ultra Low Emissions Vehicle(ULEV) standard introduced by the State of California contains an exhaust HC emissions level which is approximately 1/6 the value established by previous regulations. A major obstacle in satisfying this regulation is the unburned HC emissions exhausted before the catalytic converter is activated. Therefore, understanding the mixture preparation process during start and warm-up is very important for any possible reduction of HC emissions during that period caused by poor mixture preparation. The mixture preparation process in the intake port in a spark ignition engine depends on the thermal environment of the intake port, especially when the engine is cold. During warm-up, valve temperature goes up faster than any other engine components and a significant fraction of fuel is directly injected on the back

of the intake valve. As fuel evaporation rate heavily depends on surface temperature, it is clear that the hot valve surface will contribute to overall mixture preparation significantly during the early stage of warm-up.

In spite of its important role on the mixture preparation process, there has been no comprehensive report on the modeling of the intake valve. It is basically due to rarely available valve temperature data and the complexity of thermal environment to which the valve is exposed.

As a first step to assess the role, this study focuses on developing a heat transfer model of the intake valve under engine firing with propane. In this study, the valve is lumped into four identical elements for which the assumption of lumped thermal mass is valid. Using the four thermocouples implemented on the valve, the temperature representing each element is measured. A heat transfer model of the intake valve is developed and it is compared with the measured data. The calibration is made so that the difference between the measured and simulated valve temperatures becomes minimal. The results of the model show quantitative contribution of each heat transfer source to the overall heat balance of the valve.

When it comes to liquid fuel cases, an additional heat transfer factor which is fuel evaporation on the valve surfaces gets into the modeling. The evaporation process is hard to be modeled. From the consideration that the deficit of the heat balance for the liquid fuel case mostly comes from fuel evaporation, the amount of fuel vaporized from the valve is estimated.

2. Heat Transfer Modeling

In real engine environments, temperature

distribution in the valve is not uniform. Therefore, the intake valve needs to be divided into elements which can be approximated as lumped thermal masses. In this study, the valve consists of four identical elements. The representative temperature of each element was measured at the positions shown in Fig.1 Each element is subject to external and internal heat transfer where internal heat transfer means the heat transfer between adjacent elements. When the heat balance equations of the elements are summed up, the internal heat transfer terms are canceled out. From the consideration that the external thermal resistance is nearly independent of the valve temperature, the resultant heat balance equation becomes linear with respect to the mean of the temperatures of the elements which is the average temperature representing the valve temperature distribution. From now on, the measured valve temperature refers to the average value of the four measured temperatures.

HEAT TRANSFER MECHANISM-To simulate the valve temperature, the following heat transfer mechanisms are taken into account : 1) heat transfer from the in-cylinder charge, 2) heat transfer through valve seat and valve contact, 3) heat transfer from the forward intake flow, 4) heat transfer from the overlap backflow, 5) heat transfer from the reverse displacement flow, 6) heat transfer through the valve stem, and 7) fuel evaporation on the back of the intake valve with liquid fuel injected. Most of heat transfer coefficients can be determined from well-known experimental results, but the others, for example the heat transfer coefficient associated with valve seat and valve contact, are difficult to be predicted. To determine the unknowns, the measured valve temperature pro-

files are substituted in the heat balance equation to be described later. The idea is to find a combination of the unknowns which would produce best heat balance results for all of the test cases with a gaseous fuel. The resultant heat balance equation tells how much each heat transfer term contributes to the valve heat balance. And it is also applied to the test cases with a liquid fuel to infer the power consumed to vaporize the liquid fuel on the back of the intake valve, since any deviation from the heat balance, in that case, would be contributed by fuel evaporation which is very difficult to be modeled otherwise. The governing equation with a gaseous fuel would have the following form :

$$\begin{aligned}
 m_v C \frac{dT_v}{dt} &= \dot{q}_{cyl} + \dot{q}_{intake} + \dot{q}_{back} + \dot{q}_{seat} + \dot{q}_{stem} \\
 &= (hA)_{cyl}(T_{gas} - T_v) + (hA)_{intake}(T_{intake} - T_v) \\
 &+ (hA)_{back}(T_{gas} - T_v) + (hA)_{seat}(T_{port} - T_v) \\
 &+ (hA)_{stem}(T_{coolant} - T_v) \quad (1)
 \end{aligned}$$

LUMPED MASS-For the assumption of lumped thermal mass to be valid, the following Biot number, Bi, should be small enough.

$$Bi = \frac{L/k_s A}{1/\bar{h}_c A} = \frac{\bar{h}_c L}{k_s} \quad (2)$$

More exact analysis of transient thermal response of solids indicate that, for bodies resembling a plate, cylinder, or sphere, $Bi < 0.1$ ensures that the temperature at the center will not differ from that at the surface by more than 5%³⁾; thus, $Bi < 0.1$ is a suitable criterion for lumped thermal mass. With regard to the elements of the intake valve, there are two characteristic lengths. One is half a radius of the valve, L_r (7.5mm), and the other is half a thickness of the valve, L_t (2.5mm). Applica-

tion of the criterion led to the maximum allowable heat transfer coefficients as follows : $\bar{h}_c(\text{with } L_v) = 850 \text{ W/m}^2\text{C}$, and $\bar{h}_c(\text{with } L_v) = 2,560 \text{ W/m}^2\text{C}$. Heat transfer coefficients on the intake valve needs to be checked to see if the lumped thermal mass assumption is valid. Since the values are not known yet, the validity will be discussed after the heat transfer model is developed.

3. Experiment

TEST ENGINE-A production Volvo engine (B5254FS) was modified to fit in with the Ricardo Hydra single cylinder engine mount. The engine has two intake and two exhaust valves. Its displacement volume and compression ratio are 487.0cm^3 and 10.1, respectively. Air flow rate into the engine was measured with a laminar flow meter. The engine can be fueled with gaseous fuels and liquid fuels. Fuel metering is achieved by monitoring the equivalence ratio measured in the exhaust port with a Horiba lambda meter. Cylinder pressure was measured using the transducer manufactured

by Kistler Co.(Type 6121).

THERMOCOUPLES INSTALLATION-Fig.1 shows the thermocouples installation. Four thermocouples were spot-welded on the intake valve back and tied on the valve stem. Since the intake valve didn't rotate due to excessive valve spring force, it was possible to measure the temperatures at fixed positions. The temperatures of the two positions near the valve seat were measured using surface type thermocouples flush-mounted on the wall.

ENGINE OPERATING CONDITIONS-For the measurements, the engine was operated under the following test conditions for propane(gaseous fuel) and indolene(liquid fuel) : intake manifold pressures of 0.40, 0.62 and 1.0 bar at 1,600r/min, of 0.59 and 1.0 bar at 2,400r/min, of 1.0 bar at 3,200r/min. The engine was motored at a specified condition until the coolant temperature reached a desired low temperature(about 25°C), then it was fired until the coolant temperature reached 80°C .

4. Determination of Heat Transfer Coefficients

HEAT TRANSFER TO THE VALVE FROM IN-CYLINDER CHARGE-Heat transfer to the valve from the in-cylinder charge is a major heat source. Since the heat transfer mechanism is fundamentally the same as that on the combustion walls, Woschni's correlation⁴⁾ was assumed to be valid for this case. Woschni assumed a correlation of the form $Nu = 0.035 Re^m$ based on the flatplate forced convection heat-transfer correlation formula. Woschni's correlation converted in terms of engine parameters is represented as :

$$h_{\text{Woschni}}(\text{W/m}^2\text{K}) = 3.26 B(m)^{-0.2} p(\text{kPa})^{0.8} T(\text{K})^{-0.5} w(\text{m/s})^{0.8} \quad (3)$$

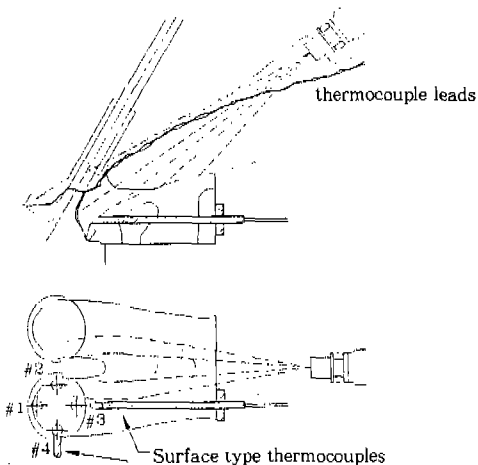


Fig.1 Thermocouples Installation and Fuel Injection Geometry

where the average cylinder gas velocity w (m/sec) determined for a four-stroke, water-cooled, four-valve direct injection CI(Compression Ignition) engine without swirl is expressed as follows :

$$w = C_1 \bar{S}_p + C_2 \frac{V_d T_r}{p_r V_r} (p - p_m) \quad (4)$$

where V_d is the displaced volume, p is the instantaneous cylinder pressure, p_r , V_r , T_r are the working-fluid pressure, volume, and temperature at some reference state(say, inlet valve closing or start of combustion), and p_m is the motored cylinder pressure at the same crank angle as p . C_1 and C_2 are empirical constants. Since the heat transfer coefficient on the combustion chamber walls may vary depending on test engine type⁵⁾, a multiplication factor K_{cyl} was introduced.

$$h_{cyl} = K_{cyl} h_{Woschni} \quad (5)$$

HEAT TRANSFER THROUGH VALVE AND VALVE SEAT CONTACT—There exists contact resistance between the valve and the valve seat when the intake valve is closed. Data for contact resistance are, unfortunately, sparse and unreliable because surface roughness is too irregular to be represented by a couple of parameters and the properties of the material filling the voids between two contacting surfaces affect thermal resistance significantly. Furthermore, there is no experimental data available for the case in study. Therefore, the contact resistance associated with the valve seat and valve contact, h_{cns} , is unknown. The unknown will be determined later by comparing the heat transfer model with measured valve temperature profiles.

HEAT TRANSFER OVER THE VALVE BACK—Since the forward flow into the cylin-

der is not steady, heat convection should be calculated based on instantaneous mass flow rates. Furthermore, complicated geometry of that region precludes any theoretical analysis. An experimental heat transfer correlation is proposed as follows by reproducing the experimental results conducted by Kapadis⁶⁾ and Engh.⁷⁾

$$Nu = 0.2 Re_D^{0.7} = 0.2 \left(\frac{\rho V D}{\mu} \right)^{0.7} \quad (6)$$

where $Re_D (= \rho V D / \mu)$ is Reynolds number. V and D represent air velocity in the intake port and valve diameter, respectively.

HEAT TRANSFER DURING VALVE OVERLAP—Near the end of the exhaust process, there is a brief period (about 20 degree in crank angle) when both the intake and exhaust valves are open before the exhaust valve closes. It is called 'valve overlap' period during which the cylinder pressure is nearly equal to the pressure in the exhaust port. Since the intake pressure is lower than the cylinder pressure at part engine load, the hot gas in the cylinder flows back into the intake port. Caton studied the case⁸⁾. He assumed the mean flow through the valve opening to be directed at the valve stem. At least locally, then, stagnation point flow was anticipated with corresponding high heat transfer rates. From that consideration, he adapted an experimental correlation for two dimensional jet impingement to model the mean heat transfer. The resultant correlation proposed by Caton is as follows.

$$Nu_{back} = \frac{h_{back} l_v}{k} = 1.2 Re_{back}^{0.58} (2l_v/D)^{0.62} \quad (7)$$

where $Re_{back} = \dot{m}_{back} l_v / (\mu A_{eff})$ and l_v is instantaneous valve lift, and D is the intake valve diameter, and A_{eff} was obtained by multiplying

instantaneous minimum valve curtain area with a discharge coefficient C_D of 0.9. The details about A_{eff} can be found in the reference.⁹⁾

HEAT TRANSFER DURING REVERSE DISPLACEMENT INTAKE FLOW—After the piston reaches 'Bottom Center'(BC) during the intake process, its upward motion results in reverse flow of the in-cylinder charge into the intake port. Since that cold reverse displacement flow resembles the hot backflow during the valve overlap, Eq. (7) holds for this case.

HEAT TRANSFER THROUGH VALVE STEM—The valve stem is exposed to two types of heat transfer mechanisms. The lower part of the stem is affected by convective heat transfer from the gas flow. Therefore, the part was assumed to be subject to the same convective heat transfer as on the back of the valve. The upper part is situated within the valve stem guide with very small gap. Since the gap is one of major engine oil leakage sources, it is assumed to be filled with engine oil. According to the specifications of the test engine, the gap is between 0.035 and 0.065mm. The mean value, 0.045mm, was used for heat transfer calculation. As the valve stem moves against the valve stem guide under the given clearance and constant pressure, the flow of the working fluid within the clearance can be assumed as a Couette flow. In that case, the temperature profile within the flow depends on the dimensionless parameter $\mu u_c^2 / K(T_1 - T_2)$, which is the Brinkman number. Since the Brinkman number is negligible in a typical range of engine speed from 300 to 6,000r/min, the viscous heating term associated with the Brinkman number is negligible. Therefore, the temperature profile in the gap is linear, as for simple conduction across a slab. In that case, the calculated heat trans-

fer coefficient was $3,200\text{W/m}^2\text{C}$. Finally it is possible to solve the heat transfer through the valve stem exposed to two types of convective heat transfer analytically.

5. Calculation of Mass Flow Rates and Gas Temperature

EXHAUST MASS FLOW RATE—Gas temperature in the cylinder is calculated from the ideal gas law, $P(\theta)V(\theta) = m(\theta)RT(\theta)$ where θ is crank angle. While $P(\theta)$ and $V(\theta)$ are known from pressure measurement and geometrical relation, respectively, it is not easy to find $m(\theta)$ since measuring instantaneous exhaust gas flow rate is difficult. For that relation, the outflow process from the cylinder is approximated as isentropic process from the fact that the actual process is close to adiabatic process.⁹⁾ In that case,

$$p(V/m)^\gamma = p(EVO)(V(EVO)/m(EVO))^\gamma \quad (8)$$

$$T = \frac{V(EVO)}{R \times m(EVO)} p(EVO)^{1/\gamma} p^{(\gamma-1)/\gamma} \quad (9)$$

$$m = \frac{pV}{RT} = m(EVO) \frac{V}{V(EVO)} \left(\frac{p}{p(EVO)} \right)^{1/\gamma} \quad (10)$$

where EVO and γ stand for exhaust valve opening and specific heat ratio, respectively. Fig.2(a) represents the instantaneous mass flow rate of the exhaust gas calculated by the isentropic model. The features of blow-down and displacement flows are well pronounced in the figure as indicated by Tabaczynski et al.¹⁰⁾

INTAKE MASS FLOW RATE—Knowledge of correct intake air flow rates into the cylinder is very important in calculating convective transfer on the back of the intake valve. A

phenomenon involved with the intake air flow is quite complicated. Several characteristics are involved in that flow. Those are backflow, forward displacement flow, backward displacement flow, and ram effect. To predict instantaneous mass flow rates accurately, the features should be taken into a flow modeling.

Backflow : Backflow occurs during valve overlap. Since the cylinder pressure is higher than the pressure in the intake port at the moment of intake valve opening, reverse flow occurs from the engine cylinder to the intake port. At the same time, the gas in the exhaust port flows back into the engine cylinder. Therefore, the phenomenon is quite complicated during valve overlap. The instantaneous reverse flows were calculated assuming an orifice flow model. The flow rate in the subsonic regime is expressed as follows :

$$\frac{dm}{dt} = \frac{C_0 A_T p_0}{\sqrt{RT_0}} \left(\frac{p_T}{p_0}\right)^{1/\gamma} \left\{ \frac{2\gamma}{\gamma-1} \left[1 - \left(\frac{p_T}{p_0}\right)^{(\gamma-1)/\gamma} \right] \right\}^{1/2} \quad (11)$$

where subscripts 0 and γ represent the stagnation condition upstream of the orifice and the condition in the orifice, respectively.

Forward displacement—After the valve overlap, the cylinder pressure becomes nearly equal to that in the intake port. In that case, the intake flow rate is approximated as a displacement flow as follows :

$$\frac{dm}{dt} \approx \frac{p_{intake}}{RT_{intake}} \frac{dV}{dt} \quad (12)$$

Reverse displacement and ram effect—When the piston moves up, it pushes some of the entrained mixture out of the cylinder by displacement motion. The phenomenon is clearly pronounced at low engine speeds. However, near the end of the intake valve closing, the

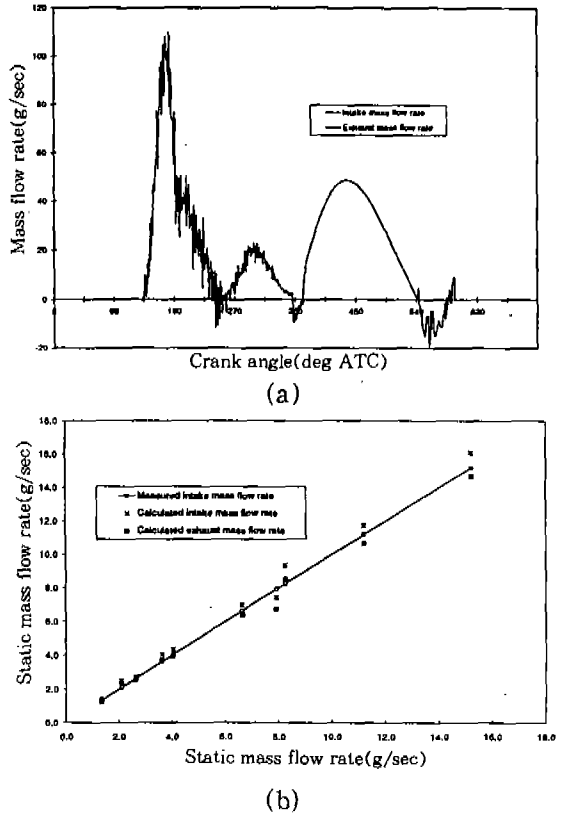


Fig.2 (a) Instantaneous Mass Flow Rates at 1,600r/min and 1.0 bar Intake Pressure, (b) Cycle-averaged Mass Flow Rates

mixture in the cylinder is inevitably compressed since the valve exit area becomes much smaller compared to the size of the displaced volume during that period. Thus, Eq. (12) doesn't hold. Furthermore, at high engine speeds, ram effect resulting from the inertial motion of fast intake air flow becomes significant. When ram effect becomes important, the intake air is not pushed out of the cylinder, but rams into the cylinder by the inertia of the fast intake flow, increasing the cylinder pressure. Since the ram effect is coupled with the compressibility of the intake air, it can not be modeled by a displacement model. Thus, a different approach is required. One possible ap-

proximation can be made in view of thermodynamic processes. During the reverse displacement flow, an isentropic process is assumed since the in-cylinder gas flows out of the cylinder nearly adiabatically. For the flow into the cylinder due to ram effects, mixing occurs between the gases in the cylinder and in the intake port. However, from the consideration that the gas temperatures are nearly the same and the proportion of that incoming air mass to the total incylinder charge is relatively small, the irreversibility associated with that mixing is neglected and hence the process is approximated as isentropic process. The resulting expressions for the entire intake process are as follows :

$$p(V/m)^{\gamma} = p(IVC)(V(IVC)/m(IVC))^{\gamma} \quad (13)$$

$$T = \frac{V(IVC)}{R \times m(IVC)} p(IVC)^{1/\gamma} p^{(\gamma-1)/\gamma} \quad (14)$$

$$m = \frac{pV}{RT} = m(IVC) \frac{V}{V(IVC)} \left(\frac{p}{p(IVC)} \right)^{1/\gamma} \quad (15)$$

where IVC stands for intake valve closing. An example of the instantaneous intake mass flow rate is shown in Fig.2(a). To confirm the validity of assuming isentropic processes, a comparison has been made among the measured intake mass flow rates and the predicted exhaust and intake mass flow rates in terms of cycle-averaged mass flow rates in Fig.2(b). The figure shows good agreement between the test data and the predicted ones. The errors among the three cases are within 10% which is tolerable to be used for convective heat transfer calculation on the valve back.

6. Calibration of the Heat Balance Equation

From the arguments made so far for the unknowns in the heat balance equation, Eq. (1), are K_{cyl} and h_{cyl} . The variables were found by adjusting them until the simulated valve temperatures of Eq. (1) showed best fit with all of the 9 cases of measured valve temperature profiles with the gaseous fuel (propane). The procedure is as follows. When the simulated valve temperature, T_v , in Eq. (1) is substituted with measured one, \bar{T}_v , which is essentially cycle-averaged, an error term is generated since \bar{T}_v is not the exact solution. Thus, the equation can be expressed as follows.

$$\begin{aligned} \text{Error}(t)_{\text{gas}} = m \cdot C \frac{d\bar{T}_v}{dt} - (\bar{h}A)_{cyl}(\bar{T}_{\text{gas}} - \bar{T}_v) - (\bar{h}A)_{\text{intake}} \\ (\bar{T}_{\text{intake}} - \bar{T}_v) - (\bar{h}A)_{\text{back}}(\bar{T}_{\text{gas}} - \bar{T}_v) - (\bar{h}A)_{\text{exhaust}} \\ (\bar{T}_{\text{port}} - \bar{T}_v) - (\bar{h}A)_{\text{stem}}(\bar{T}_{\text{coolant}} - \bar{T}_v) \quad (16) \end{aligned}$$

To find the values which minimize the error term, $\text{Error}(t)_{\text{gas}}$ of Eq. (16), the K_{cyl} was first perturbed around $K_{cyl}=1.0$ corresponding to the heat transfer coefficient predicted by Woschni's correlation. The trials and errors for the best fit resulted in the combination of $K_{cyl}=1.0$ and $h_{cyl}=2,750 \text{ W/m}^2\text{C}$. The meaning of $K_{cyl}=1.0$ is that Woschni's empirical correlation holds for a spark ignition engine like the test engine. This confirms Woschni and Fieger's experimental conclusions.¹¹⁾ The magnitude of the error term will be discussed later in conjunction with the case of liquid fuel.

NOISE FILTERING-To reduce the influence of the noises carried on the temperature measurements on the error term, the measured data were curve-fitted by a least-

square method in a polynomial equation with 10th order. Otherwise, the high frequency noise will be amplified in $\frac{dT_v}{dt}$ of Eq. (16). The statistics for the difference between the measured valve temperature and curve-fitted one show that the mean and standard deviation range about $-1.9 \times 10^{-12} \sim 1.5 \times 10^{-10}^\circ\text{C}$ and $0.62 \sim 1.19^\circ\text{C}$, respectively. It means that the amplitude of the noise is about 1°C and the noise is quite random around the curve-fitting line.

7. Application of the Calibrated Heat Balance Equation to the Liquid Fuel Cases

The amount of the fuel vaporized on the valve back is difficult to be quantified since the heat transfer takes place in transient two-phase flow and the liquid fuel consists of many hydrocarbon components. However, as far as the heat balance of Eq. (16) is accurate enough to predict the valve temperature behavior of the gaseous fuel case with minimal errors, it can be applied to the liquid fuel case as follows. For the liquid fuel case, a fuel evaporation term is added to Eq. (16).

$$\begin{aligned} \dot{q}_{\text{evap}} + \text{Error}(t)_{\text{liquid}} = & m_v C \frac{dT_v}{dt} - (\bar{h}A)_{\text{cyl}}(\bar{T}_{\text{gas}} - \bar{T}_v) - \\ & (\bar{h}A)_{\text{inake}}(\bar{T}_{\text{inake}} - \bar{T}_v) - (\bar{h}A)_{\text{back}}(\bar{T}_{\text{gas}} - \bar{T}_v) - \\ & (\bar{h}A)_{\text{scat}}(\bar{T}_{\text{port}} - \bar{T}_v) - (\bar{h}A)_{\text{stem}}(\bar{T}_{\text{coolant}} - \bar{T}_v) \end{aligned} \quad (17)$$

And \dot{q}_{evap} can be expressed in terms of the mass fraction vaporized from the valve, χ_{evap} with respect to the amount of fuel injected, as follows.

$$\chi_{\text{evap}} = \frac{m_{\text{evap}}}{m_{\text{injected}}} = \frac{-q_{\text{evap}}}{m_{\text{injected}}\{h_{\text{fg}} + C_{\text{fuel}}(T_{\text{sat}} - T_{\text{fuel}})\}} \quad (18)$$

Then, Eq. (17) is rewritten in terms of χ_{evap}

$$\begin{aligned} \dot{\chi}_{\text{evap}} + e(t)_{\text{liquid}} = & \left\{ m_v C \frac{dT_v}{dt} - (\bar{h}A)_{\text{cyl}}(\bar{T}_{\text{gas}} - \bar{T}_v) - (\bar{h}A)_{\text{inake}} \right. \\ & (\bar{T}_{\text{inake}} - \bar{T}_v) - (\bar{h}A)_{\text{back}}(\bar{T}_{\text{gas}} - \bar{T}_v) - (\bar{h}A)_{\text{scat}}(\bar{T}_{\text{port}} - \bar{T}_v) \\ & \left. - (\bar{h}A)_{\text{stem}}(\bar{T}_{\text{coolant}} - \bar{T}_v) \right\} / \left\{ m_{\text{injected}} \{ h_{\text{fg}} + C_{\text{fuel}}(T_{\text{sat}} - T_{\text{fuel}}) \} \right\} \end{aligned} \quad (19)$$

where

$$e(t)_{\text{liquid}} = \frac{\text{Error}(t)_{\text{liquid}}}{m_{\text{injected}}\{h_{\text{fg}} + C_{\text{fuel}}(T_{\text{sat}} - T_{\text{fuel}})\}} \quad (20)$$

Similarly Eq. (16) also can be expressed in terms of χ_{evap} although there is no fuel evaporation for the gaseous fuel case. Then, $e(t)_{\text{gas}}$ is defined as follows :

$$e(t)_{\text{gas}} = \frac{\text{Error}(t)_{\text{gas}}}{m_{\text{injected}}\{h_{\text{fg}} + C_{\text{fuel}}(T_{\text{sat}} - T_{\text{fuel}})\}} \quad (21)$$

where the saturation temperature, T_{sat} , was calculated from a gasoline model developed by Chen et al.¹²⁾ In that model, real gasoline was represented by 13 major hydrocarbon species so that the characteristic distillation curve of a gasoline model matches with that of the real gasoline. According to the gasoline model, the saturation temperature ranges from 80 to 105 °C depending on the intake manifold pressure. The definition of $e(t)_{\text{gas}}$ facilitates direct comparison of the two fuel types for the same engine test condition. For the gaseous fuel, only the error term, $e(t)_{\text{gas}}$, will show up in Eq. (16), since χ_{evap} is equal to zero. If $e(t)_{\text{gas}}$ is small enough to be neglected, χ_{evap} can be estimated from Eq. (17) by neglecting $e(t)_{\text{liquid}}$ from the assumption that $e(t)_{\text{liquid}}$ would be in the same order of $e(t)_{\text{gas}}$. Fig.3 shows calculated results of $e(t)_{\text{gas}}$ and χ_{evap} during warm-up periods. Standard deviation of $e(t)_{\text{gas}}$ was

less than 3%. Thus, same degree of errors in χ_{evap} is expected.

8. Factors Affecting the Accuracy of the Mass Fraction Vaporized, χ_{evap}

Fundamentally the accuracy depends on that of Woschni's correlation of Eq. (3) and the validity of the assumption of lumped thermal mass.

SENSITIVITY TO WOSCHNI'S CORRELATION-According to some experimental results,⁵⁾ the heat flux from the in-cylinder gas to the combustion chamber wall shows large degree of spatial and cyclic variations. To take this fact into account, the sensitivity of K_{cyl} to χ_{evap} was investigated. Although the best fit was made at $K_{\text{cyl}}=1.0$, the cases of $K_{\text{cyl}}=0.9$ and 1.1. were also compared. Fig.3 shows an example of χ_{evap} comparing the three cases. According to the result, it is observed that χ_{evap} is proportional to K_{cyl} . Therefore, when the bound of uncertainty in K_{cyl} is assumed as 10%, the same value is also expected in χ_{evap} .

VALIDITY OF LUMPED THERMAL MA-

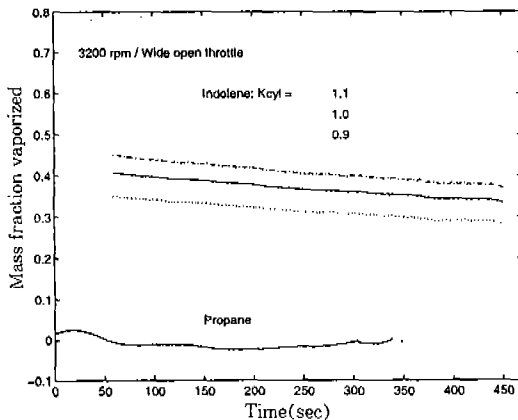


Fig.3 Sensitivity of K_{cyl} to the Mass Fraction Vaporized, χ_{evap}

SS-From the previous consideration about the criterion of Bi number for the assumption of lumped thermal mass, the maximum allowable heat transfer coefficient in the radial direction and that in the axial direction were $850\text{W/m}^2\text{ }^\circ\text{C}$ and $2,560\text{W/m}^2\text{ }^\circ\text{C}$, respectively. According to the calibrated heat balance equation for the gaseous fuel, the heat transfer coefficient on the front face by the in-cylinder charge is $78\sim 355\text{W/m}^2\text{ }^\circ\text{C}$, and the value on the valve seat is $930\text{W/m}^2\text{ }^\circ\text{C}$, and the value on the back of the intake valve by the forward intake flow is $17\sim 119\text{W/m}^2\text{ }^\circ\text{C}$ over the tested conditions. The heat transfer coefficients are summarized in Table 1. Since the heat transfer coefficient on the valve seat, $930\text{W/m}^2\text{ }^\circ\text{C}$, is comparable to the maximum allowable value in the radial direction, $850\text{W/m}^2\text{ }^\circ\text{C}$, the elements meet the Bi number criterion in the radial direction.

The criterion is also satisfied in the axial direction as the maximum value of the heat transfer coefficient on the front and back surfaces for the valve, $355\text{W/m}^2\text{ }^\circ\text{C}$, is much less than the critical value in the axial direction, $2,560\text{W/m}^2\text{ }^\circ\text{C}$. Therefore, the elements of the valve satisfy the assumption of lumped thermal mass. Fig.4(a) shows an example of measured valve temperatures for the gaseous fuel.

Table 1 List of Heat Transfer Coefficients Associated with Valve Heat Transfer

heat transfer coefficient, h	value ($\text{W/m}^2\text{ }^\circ\text{C}$)
axial direction of valve head(for lumped mass assumption)	850
radial direction of valve head(for lumped mass assumption)	2,560
front valve face by the in-cylinder gas	$78\sim 355$
valve seat	930
valve back by forward flow	$17\sim 119$

The reason why the measurement positions show different temperature behavior in spite of the axially symmetrical geometry of the intake valve can be explained by the following two considerations. According to the calibrated heat balance equation, the average heat transfer coefficient for the valve seat and valve contact, $930\text{W/m}^2\text{C}$, is a little larger than the critical value in the radial direction, $850\text{W/m}^2\text{C}$, so it could affect the temperature distribution in the radial direction. In addition, the contact resistance also could be unevenly distributed along the valve lip since the valve doesn't rotate.

When it comes to the liquid fuel case, fuel

evaporation causes the significant cooling of the intake valve. Fig.4(b) shows an example of the measured temperatures. Positions #2 and #3 show lower values than the others due to direct fuel impingement. It is because the positions #2 and #3 are located under the footprint of the fuel spray as shown in Fig.1. It is necessary to check if the assumption of lumped thermal mass is valid under the fuel injection. The temperature difference between the front and back surfaces can be estimated from heat balance consideration. According to the results of the calibrated heat balance(refer to Fig.5(a)), the cycle-averaged power taken by fuel evaporation is about 80W at $3,200\text{r/min}$. If it is assumed that fuel evaporation occurs over half the valve area, the temperature difference across the thickness of the valve face would be about 4C . It is small enough for the assumption of lumped thermal mass in the axial direction. When it comes to the radial direction, there is uncertainty in effective fuel wetting area. Considering the normal distribution of droplets population and the distance of about 10cm between the valve surface and the injector tip, the effective wetting area is larger than the valve area covered by the footprint as shown in Fig. 1 and the droplets population would be relatively uniform. Furthermore, the order of the penetration depth within which 5% of temperature deviation(for lumped thermal mass assumption) is observed would be a few millimeter from the boundary of the effective fuel wetting area. When those factors are taken into account, the measured temperature at each element can be approximated as a representative temperature for the element. Since it is an approximation, it may cause significant errors when the contribution of fuel evaporation to the heat balance is small, in other

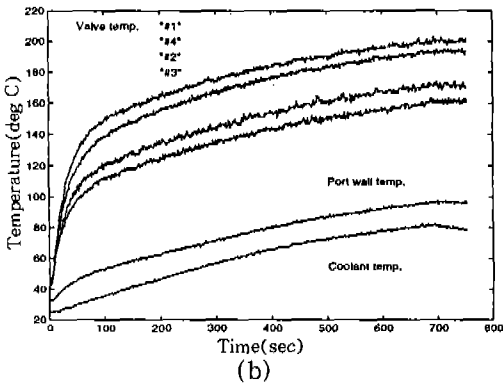
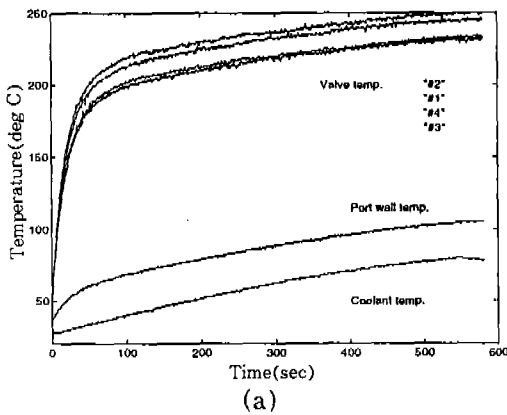


Fig.4 Measured Temperature Profiles at 1,600r/min and 1.0 bar of Intake Pressure, for (a) Propane, (b) Indolene

words, when fuel consumption rate is small.

IMPACT OF TRANSIENT VALVE TEMPERATURE-The assumption of lumped thermal mass, however, is not effective for the first 30 to 60 seconds during which the measured temperature gradient was smaller than the gradient of simulated temperature. The discrepancy is due to the assumption of lumped thermal mass. In reality, liquid fuel is impinged on the thermocouple position at the valve back and it takes awhile for temperature gradient to propagate through the valve head. Therefore, the measured temperature kicks off more slowly than the simulated temperature. The time derivative of the temperature difference term has a significant impact on the estimation of fuel mass vaporized off the valve. Therefore, the results of the heat transfer model is meaningful after the transient valve temperature term becomes negligible. Furthermore, according to Martins et al¹⁵⁾, the existence of liquid fuel on the valve surfaces significantly affects the heat transfer through the valve seat and valve contact. It is difficult to determine how long liquid fuel exists on the valve surfaces, but as a rule of thumb 60 seconds would be a good approximation since the valve temperature will be above boiling temperature by then from the argument to follow. Thus, in this study, the calculated mass fraction χ_{vap} is assumed to be valid after 60 seconds since engine start.

9. Results of Heat Balance

Fig.5(a) represents the heat balance results for the gaseous fuel at 80°C of coolant temperature. In the figure, the heat balance was calculated for the two intake valves. Nearly all of the heat input comes from the heat transfer from the in-cylinder charge. Most significant

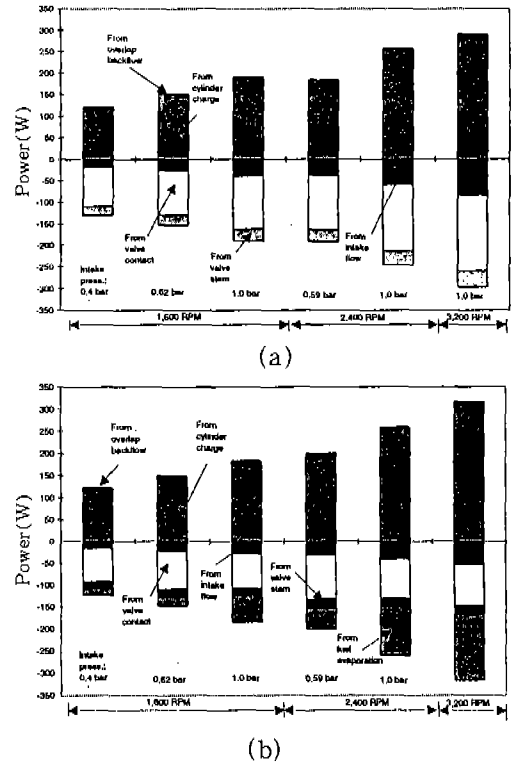


Fig.5 Results of Heat Balance for (a) Propane, (b) Indolene

heat loss is made through the valve seat and valve contact. The second largest contributor to the heat loss is the heat convection by the intake air flow. It is observed that the latter is proportional to engine speed and load as they increase air flow rate. The heat loss through the valve stem is small and relatively constant because heat flows through the small cross-section of the valve stem with small temperature gradient. Fig.5(b) shows the results of the heat balance for the liquid fuel at 80°C of coolant temperature. As engine speed and load increase, the portion of heat loss due to fuel evaporation increases. It is simply because the valve surfaces are exposed to more fuel flow rate. Therefore, at high engine speed and load, the contribution of fuel evaporation to the heat balance becomes significant.

10. Physical Interpretation of the Mass Fraction Vaporized, χ_{evap}

One common feature observed in the Fig.6 (a) to 6(c) is that the mass fraction vaporized, χ_{evap} tends to decrease with the increase of the coolant temperature.

HEAT TRANSFER REGIMES ON THE VALVE SURFACE-This can be explained by fuel evaporation behavior. The behavior is characterized by evaporation regimes such as convective heat transfer and nucleate boiling. Nucleate boiling occurs above boiling temperature and is very efficient in fuel evaporation. It is not possible to determine a single boiling temperature of gasoline at a given pressure, since gasoline is a mixture of many hydrocarbon components. However, if gasoline is modeled as a mixture of a few major hydrocarbon components so that it represents real gasoline, it is possible to do thermodynamic analysis using the gasoline model. Such a model was proposed by Chen et al¹²⁾. It consists of 13 major hydrocarbon species and their compositions are adjusted so that the model simulates the distillation curve of real gasoline. Saturation vapor pressure of the fuel was obtained using the simulation program for calculation of thermodynamic equilibrium, STRAPP, released by NIST. It includes a database of 116 components, mostly hydrocabons, performs phase equilibrium calculations by Peng-Robinson equation of state¹³⁾, and calculates thermodynamic properties of components of both vapor and liquid phases. According to the results of the program, the boiling temperature ranges from 80 to 105°C for the intake manifold pressure from 0.4 bar to 1.0 bar. Since the valve temperature rises quickly to the boiling temperature range in about 30 to 60 seconds, evaporation is in the nucleate boil-

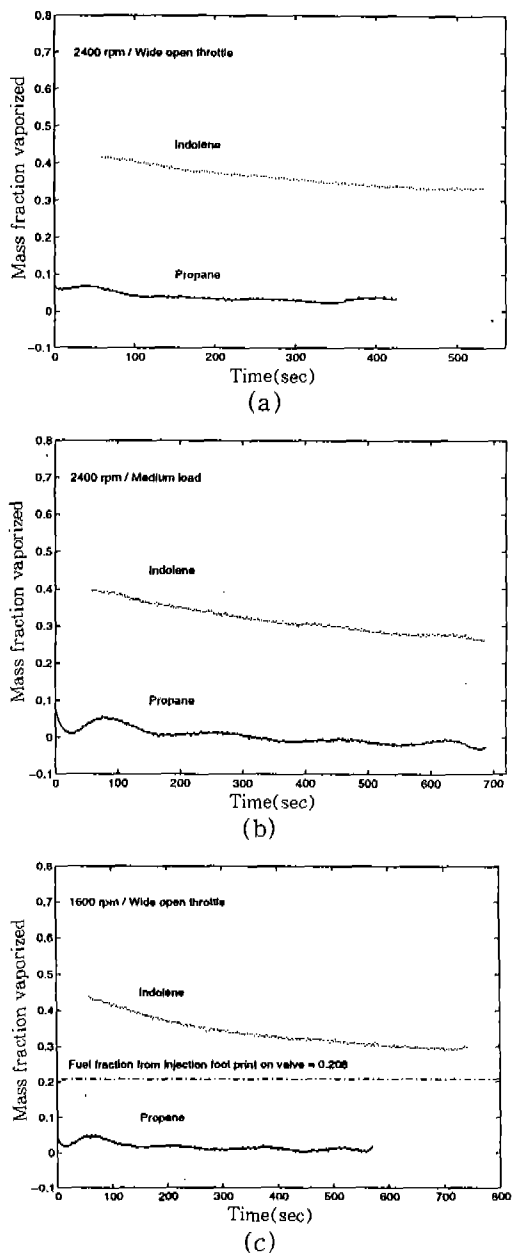


Fig.6 Calculated Mass Fraction, χ_{evap} (a) 2,400r/min, 1.0 bar, (b) 2,400r/min, 0.59 bar, (c) 1,600r/min, 1.0 bar

ing regime after that. According to Martins and Finlay¹⁴⁾, nucleate boiling was observed at the temperatures between 100 and 220°C

through visual inspection of fuel film on the valve back and from power consumption data. Beyond 220°C, film boiling was observed which is less effective than nucleate boiling. On the other hand, convective fuel evaporation occurs on the port walls during most of warm-up period since the port wall temperature is below 100°C. Under the circumstance, fuel evaporation rate is dependent upon the port wall temperature and air flow rate over the walls.

EFFECT OF FUEL TRANSPORT MECHANISM—The behavior of the mass fraction vaporized, χ_{evap} , is related with fuel transport mechanism in the intake port. Some of the injected fuel is directly targeted to the back of the intake valve from the fuel injection geometry as shown in Fig.1. The fraction of the footprint overlaid with the valve is about 20%. And about 10 to 20% of the injected fuel evaporates directly from the fuel spray according to the simulation results by Finlay¹⁵). Therefore, the rest of the injected fuel (about 60 to 70%) hits the port walls. At low coolant temperatures, most of the fuel landing on the port walls survives the evaporation process on the port walls and is transported to the intake valve in either film flow or small droplets bouncing off the port walls. All of the liquid fuel arriving at the valve evaporates quickly due to vigorous boiling evaporation. This is the reason why the mass fraction vaporized is higher at low coolant temperatures. With the increase of coolant temperature, the fuel evaporation on the port walls becomes vigorous, so less amount of the liquid fuel is transported to the intake valve. It results in less amount of the fuel vaporized from the valve back. This explains the tendency of the decreasing fuel fraction vaporized with the increase of the coolant temperature. Quantitatively, the mass

fraction vaporized has its maximum of about 40 to 45% at around 100 seconds since engine start.

BEHAVIOR OF FUEL FRACTION VAPORIZED AT WARMED-UP CONDITIONS—Another feature observed in Fig.6(a) to 6(c) is the physical meaning of the fuel fraction vaporized at 80°C of the coolant temperature. The fraction is plotted with respect to fuel consumption rate in Fig.7. At that temperature, the port walls are near the nucleate boiling regime, thus most of the liquid fuel hitting the port walls evaporates as soon as it hits the walls. At low engine speed where more time is available for fuel evaporation, and at low engine load where less amount of fuel injection results in wider fuel evaporation area, nearly all of the fuel landing on the port walls evaporates. Thus, the fraction of the fuel vaporized from the valve back becomes close to the fraction directly landing on the valve back from the fuel injection geometry (about 20%) as shown in Fig.1. Whereas at high engine speed and load, some portion of the liquid fuel landing on the port walls is transported to the intake valves due to less available time for fuel evaporation time.

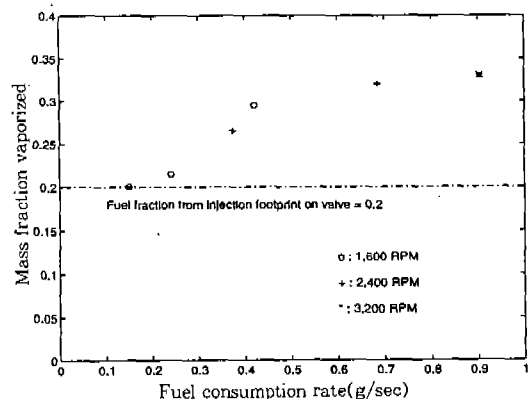


Fig.7 Mass Fraction Vaporized, χ_{evap} vs. Fuel Consumption Rate at 80°C of the Coolant Temperature

11. Conclusions

It was possible to develop a heat transfer model of the intake valve based on the assumption of lumped thermal mass under the transient engine environments during engine warm-up. Some unknowns of the model were determined by calibrating the model with the measured valve temperature profiles for the gaseous fuel.

The results of the model show quantitative contribution of each heat transfer source to the heat balance of the intake valves. It is noted that the heat loss through the valve seat and valve contact is most significant. For the liquid fuel, the heat loss due to fuel evaporation becomes dominant as engine speed and load increase since the increased fuel flow rate takes more heat off the intake valves.

The tendency that the fuel fraction vaporized from the valve back decreases as the coolant temperature increases explains how fuel evaporation occurs in the intake port during engine warm-up. At low coolant temperatures, most of the liquid fuel on the port walls is transported to the valve back and evaporates there by nucleate boiling, leading to the higher fraction of the fuel vaporized than at higher coolant temperatures. The fraction of the fuel vaporized at 80°C of the coolant temperature at low engine speed and load is close to the fraction expected from the footprint of the fuel spray. It means that most of the liquid landing on the port walls evaporates on the walls without being transported to the intake valves.

References

1. Fozo and C. Aquino, Transient A/F characteristics for cold operation of a 1.6 liter engine with sequential fuel injection, SAE Paper 880691(1989).
2. K. Horie, H. Takahasi, and S. Akazaki, Emissions reduction during warm-up period by incorporating a wall-wetting fuel model on the fuel injection strategy during engine starting, SAE Paper 952478 (1995).
3. A. F. Mills, Heat transfer, pp.29~37, Irwin, Boston, MA(1992).
4. G. Woschni, Universally applicable equation for the instantaneous heat transfer in the cylinder of a high speed diesel engine. SAE paper 670931, SAE *Trans.*, vol.76 (1967).
5. A. C. Alkidas, Heat transfer characteristics of a spark ignition engine, *J. Heat Transfer*, vol. 102, pp.189~193(1980).
6. D. N. Kapadia and G. L. Borman, The effect of heat transfer on the steady flow through a poppet valve, SAE paper 670479(1967).
7. G. T. Engh and C. Chiang, Correlation of convective heat transfer for steady intake-flow through a poppet valve, SAE paper 700501(1970).
8. J. A. Caton and J. B. Heywood, An experimental and analytical study of heat transfer in an engine exhaust port, *Int. J. Heat Mass Transfer*, vol. 24, No. 4, pp.581~595(1981).
9. J. H. Heywood, Internal combustion engine fundamentals, McGraw-Hill Book Company, pp.164~169(1988).
10. R. J. Tabaczynski, J. B. Heywood, and J. C. Keck, Time-resolved measurements of Hydrocarbon mass flow rate in the exhaust of a spark-ignition engine, SAE paper 720112, SAE *Trans.*, vol. 81 (1972).
11. G. Woschni and J. Fieger, Experimental

- investigation of the heat transfer at normal and knocking combustion in spark ignition engines. *MTZ*, vol. 43, pp.63~67 (1982).
12. K. C. Chen, K. DeWitte, and W. K. Cheng, A speciesbased multi-component volatility model for gasoline, SAE paper 941877 (1994).
 13. D. Y. Peng and D. B. Robinson, A new two-constant equation of state, *I&EC Fu* *nd*, 15, pp.59~64(1976).
 14. J. J. G. Martins and I. C. Finlay, Heat transfer to air-ethanol and air-methanol sprays flowing in heated ducts and across heated intake valves, SAE paper 900583 (1990).
 15. J. J. G. Martins and I. C. Finlay, Fuel preparation in port-injected engines, SAE paper 920518(1992).